Upgrading the Lycoming College Vacuum Chamber for

Production of an Electron Beam and the Study of Charged Particle Dynamics

Presented to the faculty of Lycoming College in fulfillment of the requirements for Departmental Honors in Astronomy and Physics.

By

Ryan Alexander Grosso

Lycoming College

April 29, 2010

Approved by:

David G. Fisher

Dr. David G. Fisher

Chris W. Kulp

Dr. Christopher W. Kulp

Gene D Sprechini

Dr. Gene D. Sprechini

Jeremy D. Ramsey

Dr. Jeremy D. Ramsey

Table of Contents

Page Number

Table of Figures

Page Number

Abstract:

The Lycoming College Astronomy and Physics department's vacuum system was significantly upgraded as a result of this project in addition to the efforts of several previous physics students. Lab Director and Lycoming College Alumnus ('81), Jeff Garrett, of Outgassing Services International (O.S.I.) in Mountain View California, supplied many of the necessary vacuum fittings and hardware. Plasma was created to explore the acceleration of charged particle dynamics by field emission and thermionic emission. Large solenoid magnets were made and tested for compatibility with operation of the vacuum chamber. A detection system was engineered to measure the presence and energies of the particles.

Introduction:

Particle acceleration first became popular around the early 1900's. The idea was that through application of Maxwell's equations it would be possible to accelerate a charged particle to higher velocities (energies) than previously attainable. One of the most famous milestones in particle accelerator physics came in 1930 when Ernest O. Lawrence built the first cyclotron.[1] His cyclotron was one of the earliest types of particle accelerators, and that design is still used today as the first stage of some large multi-stage particle accelerators. It made use of the magnetic force on a moving charge to bend moving charges into a semicircular path between accelerations provided by an applied electric field. The applied electric field accelerated charged particles between the gaps in the dees in the magnetic field region. The dees are hollow, semicircular metal cups which the particle travels between. Lawrence's cyclotron incorporated a uniform magnetic field; this is that the vertical magnetic field is uniform in azimuth. The field magnitude was almost constant in the radial direction but varied slightly at the edges of the magnet due to bulging magnetic field lines.

<u>The cyclotron</u>

Because of the cyclic paths of the ions, this accelerator is called a cyclotron. The cyclotron operates on the principle of particle mass resonance. The device uses two hollow D-shaped electrodes, called dees, held in a vacuum between poles of an electromagnet. A high-frequency alternating current (AC) voltage is applied to each dee. In the space between the dees, an ion source generates positive ions. These ions are accelerated into one of the dees by electrostatic attraction, and when the alternating current shifts from positive to negative during each half cycle of oscillation, the ions turn and accelerate into the other dee. Due to the strong electromagnetic field, the ions travel in a circular path, their path of least resistance. Each time the ions move from one dee to another, they gain energy. This way their rotational radius increases incrementally, and they execute a spiral orbit. This acceleration continues until the ions escape from the dees. The main parameters of a cyclotron are the strength of the magnetic field, the particle charge to mass ratio, and the frequency of the AC field on the dees.[2] A beam can only be established for a particle's specific charge to mass ratio. If the frequency is not set properly, the particle will fall out of orbit and not accelerate as needed. See Figure 1.

Figure 1

Cyclotron

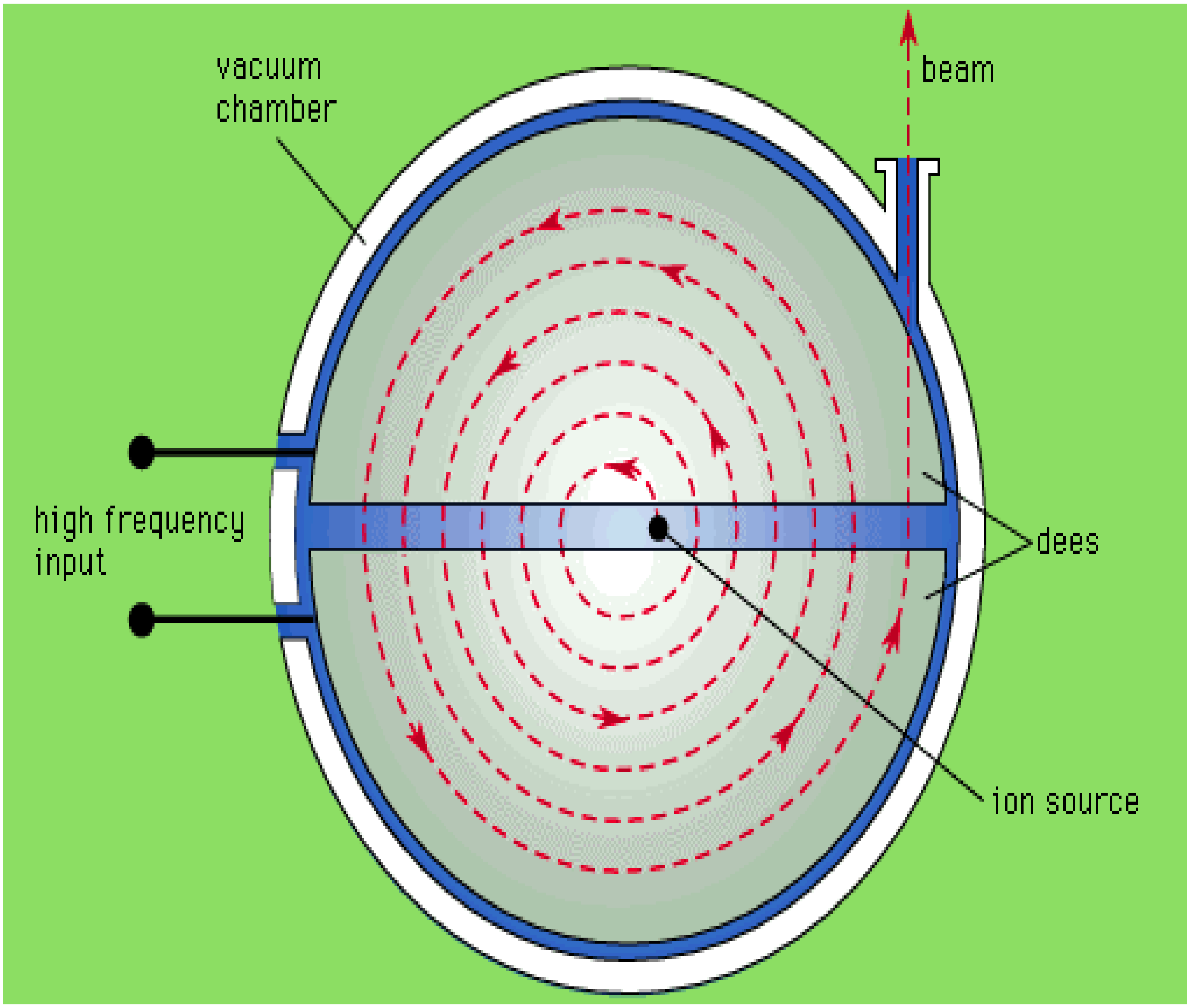

*Encyclopedia Britannica 1988

Ion Production for Cyclotrons

In a cyclotron, ions are produced in between the dees and the acceleration gap. The first proposed method is by means of a filament. A filament is a thin wire with a high current flowing through it. This high current causes the wire to heat up which in turn produces electrons or ions by means of thermionic emission. The second method uses direct ionization from an electric field. If an atom is subject to a sufficiently strong electric field, greater in electrostatic energy than the binding energy of that atom, the atom will ionize. Electrons will migrate towards the positive field pole, and the positively charged nucleus, which contains protons, will migrate toward the negative field pole. These ions then drift up into the region between the plates and begin to accelerate from forces due to the electric field produced by the dees. Particles gain energy when crossing through the potential difference between the dees, thus accelerating them. Then the particles collide into the detector, and the data is logged and recorded. The detector allows for confirmation of the beams presence and the energy of the particles.

The cyclotron frequency

It is critical to determine the frequency of the particle in the cyclotron. This frequency directly correlates to the frequency of the oscillating potential on the dee's. To calculate the cyclotron frequency for a particle to maintain a stable orbit between the dee's, the centripetal force and the magnetic force on a charged particle must be equated.

where,

$$F_c = \frac{mv^2}{r} \quad , \; F_{mag} = q(v \times B) \qquad (1.1)$$

$$\frac{mv^2}{r} = qvB \qquad (1.2)$$

where,

$$\frac{v}{r} = \omega \quad , \quad f = \frac{\omega}{2\pi} \qquad (1.3)$$

Thus,

$$m\omega = qB \xrightarrow{yields} f = \frac{qB}{2m\pi} \qquad (1.4)$$

This calculation of the cyclotron frequency will hold for non-relativistic speeds. If speeds approach that of light a relativistic form must be used. These more general, relativistic equations are commonly expressed in cylindrical coordinates.

<u>Derivation and Explanation of Forces</u>

Due to the geometry of many particle accelerators cylindrical coordinates would be the best way in deriving relativistic particle motion in cylindrical coordinates. Cylindrical coordinates are based on curved coordinate lines and denoted by (r, θ, z).
Relativistic momentum is

$$p_{rel} = \gamma m_0 v \qquad (1.5a)$$

$$\gamma \equiv \sqrt{1-\beta^2} \qquad \text{and} \qquad \beta \equiv \frac{v^2}{c^2} \qquad (1.5b)$$

The Cartesian equation of motion is

$$\frac{dp_x}{dt} = F_x \qquad (1.6)$$

So,

$$p_x = p_r \cos(\theta) - \ p_\theta \sin(\theta)\,, \qquad F_x = F_r \cos(\theta) - \ F_\theta \sin(\theta) \qquad (1.7)$$

$\binom{p_r}{p_\theta}$ is a rotation of $\binom{p_x}{p_y}$ about the angle θ

$$\binom{p_r}{p_\theta} = \begin{pmatrix} \cos\theta & -\sin\theta \\ \sin\theta & \cos\theta \end{pmatrix} \binom{p_x}{p_y} \qquad (1.8)$$

Refer to Figure 2

Figure 2

Cartesian and Cylindrical Coordinates & Momentum Components

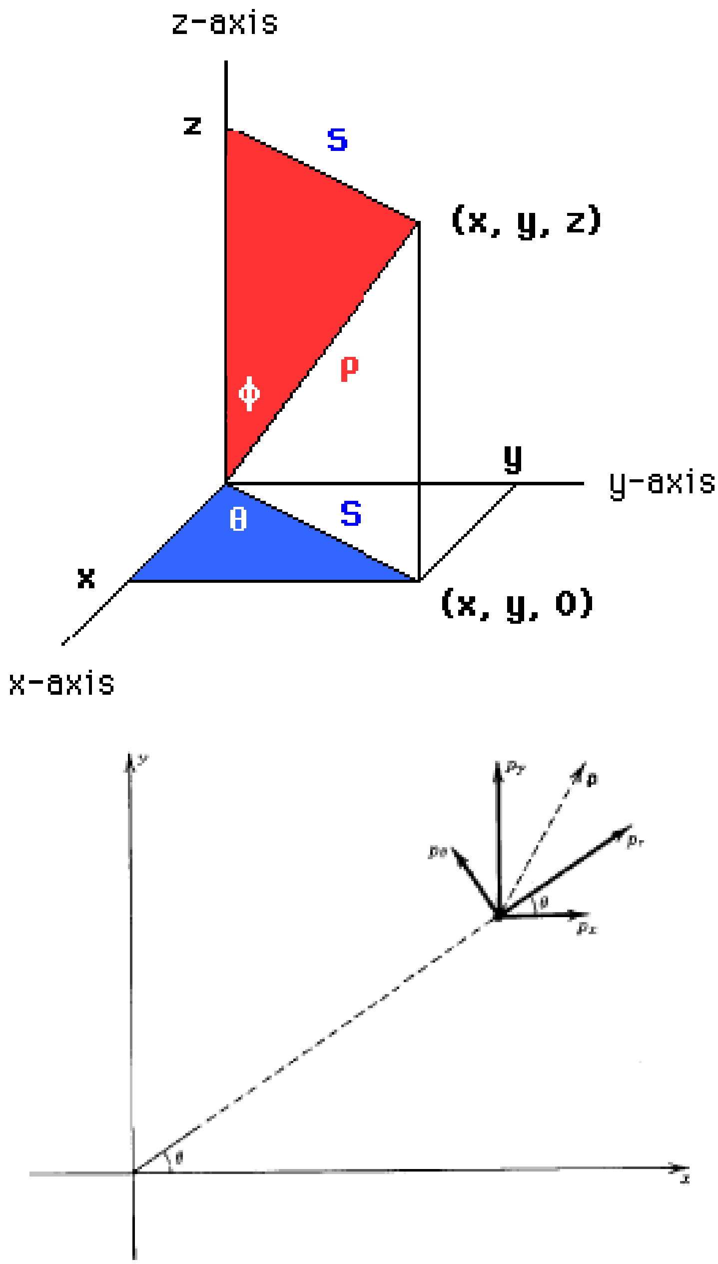

*http://www.math.montana.edu/frankw/ccp/multiworld/multipleIVP/spherical/convert3d.gif

Now substitute Eq. (1.7) into Eq. (1.6)

$$\frac{dp_r}{dt}\cos(\theta) - p_r\frac{d\theta}{dt}\sin(\theta) - \frac{dp_\theta}{dt}\sin(\theta) - p_\theta\frac{d\theta}{dt}\sin(\theta) = F_r\cos(\theta) - F_\theta\sin(\theta) \quad (1.9)$$

Separating the Trigonometric factors (Sin θ, Cos θ) one finds:

$$\frac{dp_\theta}{dt} = F_\theta - \{p_r\frac{d\theta}{dt}\} \quad (1.10a)$$

$$\frac{dp_r}{dt} = F_r + \{p_\theta\frac{d\theta}{dt}\} \quad (1.10b)$$

Equations (1.10a) and (1.10b) are very similar to the Cartesian Newtonian equations of motion. The bracketed terms are considered as "correction terms" for using cylindrical coordinates. The bracketed term in equation (1.10a) is a "fictitious" or virtual force referred to as the Coriolis force. Using the relativistic momentum we can obtain the relativistic form of the Coriolis force.

$$Coriolis\ Force = -p_{r,rel}\left(\frac{d\theta}{dt}\right) = -\frac{\gamma m_0 v_r v_\theta}{r} \quad (1.11)$$

The bracketed term in equation (1.10b) is also a "fictitious" or virtual force referred to as the Centrifugal force. Using the relativistic momentum one can obtain the relativistic form of the centrifugal force.

$$Centrifugal\ Force = p_{\theta,rel}\left(\frac{d\theta}{dt}\right) = \frac{\gamma m_0 v_\theta v_\theta}{r} = \frac{\gamma m_0 {v_\theta}^2}{r} \quad (1.12)$$

For low energies the non relativistic form can be used to approximate the frequency of the particle.

$$f = \frac{qB}{2m\pi} \quad (1.13)$$

Approaching speeds close to that of light the relativistic frequency must be used.

$$f = \frac{qB}{2\pi\gamma m_0} \quad (1.14)$$

Experimental Overview:

This thesis reports on the upgrade of the Lycoming College vacuum chamber including design and installation of parts. It explains the engineering of parts in which ions were produced, such by field emission and thermionic emission. It was observed that a point source ion source produces an unstable beam and discharges to its closest ground. This led to development and construction of a custom designed magnetic and electric field system configuration. With a controlled ion beam a detection system was devised to detect the beam's presence.

Vacuum Chamber:

Pumping Mechanism

The main pump that is used to evacuate the chamber from atmospheric pressure is mechanical Duo-Seal Vacuum Pump. This is a roughing pump that can optimally spin at 300 revolutions per minute. The pump is connected to a DV foreline trap by a rubber hose 8.0 cm in length, having an outer diameter of 3.0 cm and an inner diameter of 1.5 cm. The top of the trap connects via a flange (part number KF NW-25) to a stainless steel bellows. The long bellows and foreline trap are to help avoid any small particle or oil residue from reentering the chamber. The bellows then connected to a flange (part number NW-25) which directly allowed the chamber to be open and closed by a valve. A conflate liquid nitrogen trap was donated from Lycoming College Alumnus Jeff Garrett Class ('81). This was installed between the bellows and NW-25 chamber valve. When the trap is filled with liquid nitrogen it allows for more particles to attach to the trap surface and not bounce back into the chamber, this effect thus lowers the pressure in the chamber.

Chamber Entry Flanges.

The Lycoming College vacuum chamber consists of eight flanges on the side of the chamber walls. The flanges allow for manipulation and changes to occur in the inside of the chamber while the chamber is running below atmospheric pressure. The flange points are set, if viewed from above, to be numbered ascending clockwise starting with the flange connecting to the pump as defined as flange 1. Refer to Figure 3.

Figure 3

Chamber Entry Flanges

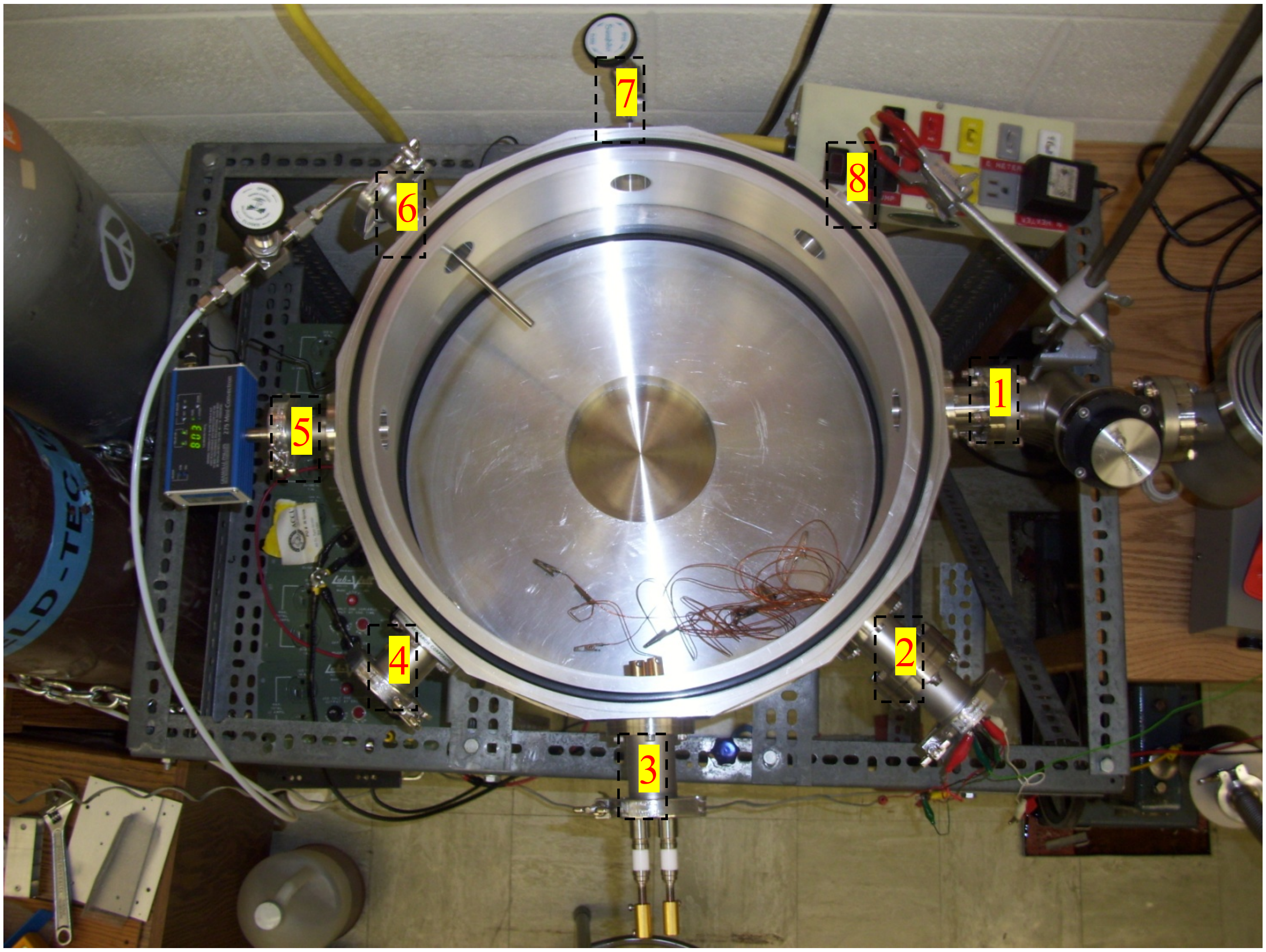

Flange style and connections

1. A conflate flange that connect and LN2 trap which then connects to the mechanical pump. *
2. A conflat flange that adapts from a conflat to a flange part number IFT-NW-40-8P electrical feed which has eight pin connections that are each .032” OD nickel wire rated for 500VDC at 2 Amps. *
3. A KF flange that connects to a flange part number MCF-NW-40-2 medium current copper electrical feedthrough which has two pins that are each .25” OD OFHC copper wire rated for 5KVDC at 150 Amps.*
4. A KF flange part number NW-40 blank *
5. A KF flange part number NW-25 connects to a Granville Phillips 275 Mini Convectron module which is a digital thermocouple gauge control which allows a precise pressure reading at any given moment within the range of 800 Torr – 10 mTorr.*
6. A KF flange part number NW-40 connects to a flange part number 2NR-NW-40-25 which then connects backwards to another flange part number 2NR-NW-40-25 which then connects to custom made flange part number KF NW-40 gas leak. *
7. A custom made Swagelok fitting which allows venting of the chamber. *
8. A direct blank on the chamber.

*Donated from alumnus Mr. Jeff Garret ‘81

Figure 3a

Flange 1

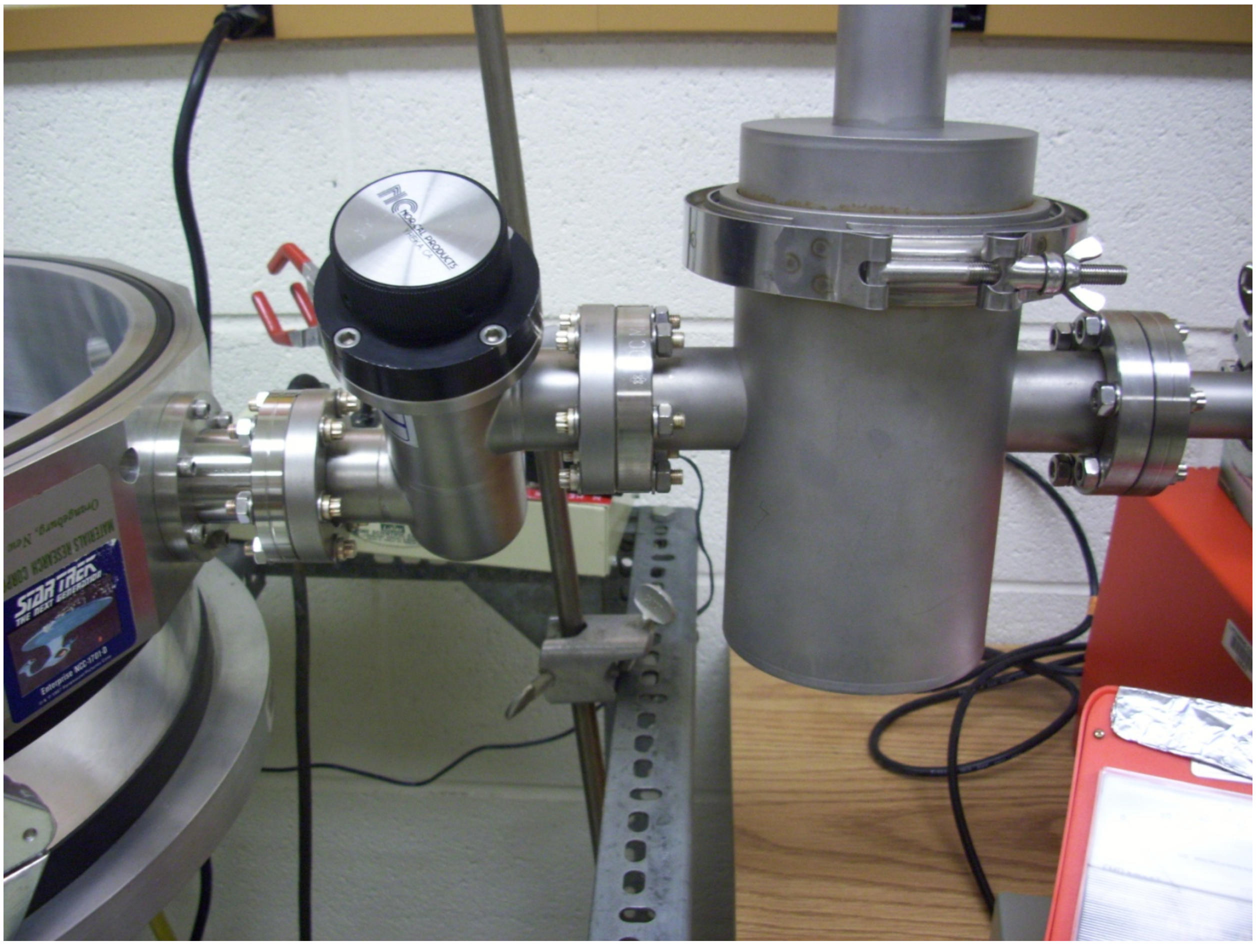

LN2 Trap

Figure 3b

Flange 2

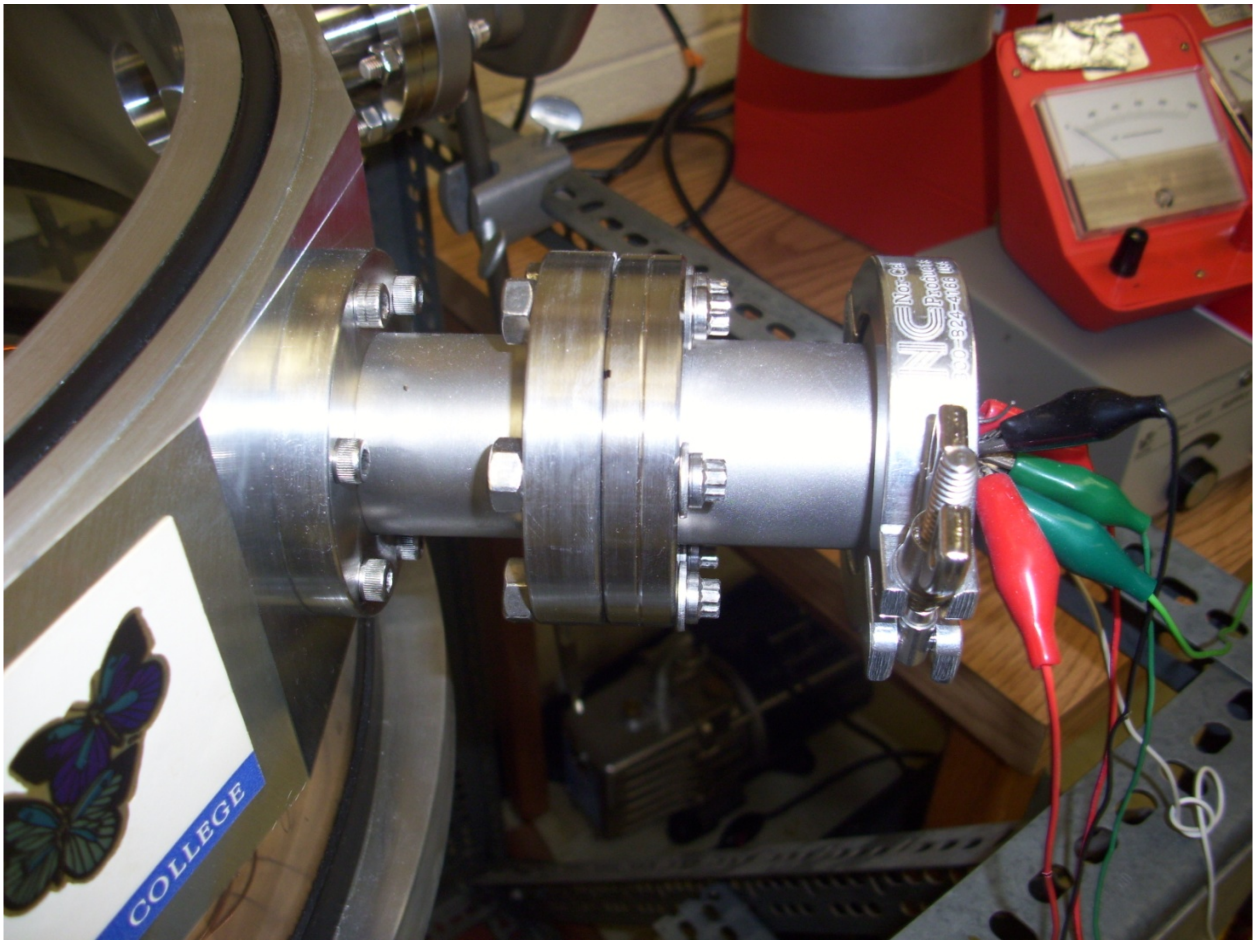

IFT-NW-40-8P electrical feed

Figure 3c

Flange 3

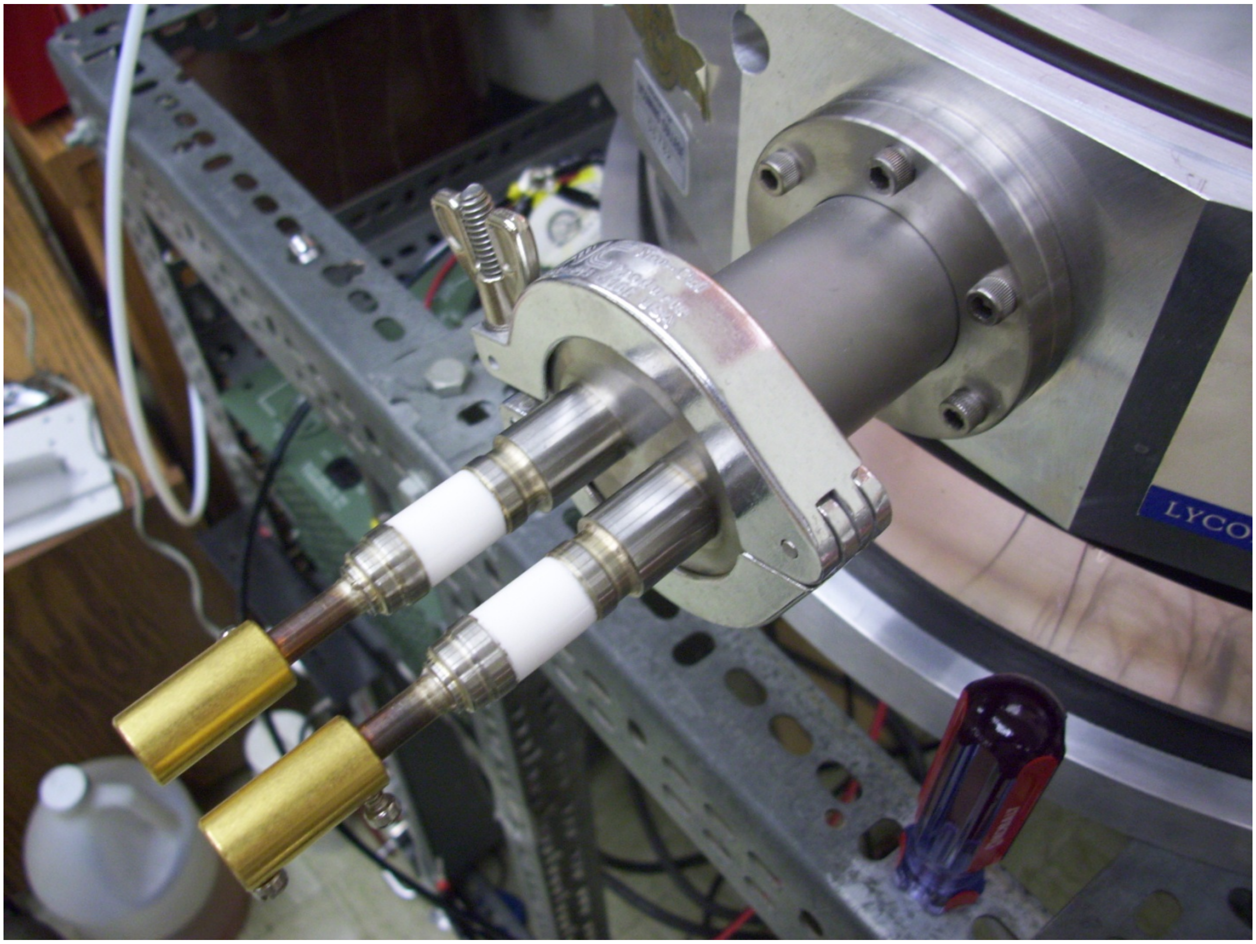

MCF-NW-40-2 electrical feedthrough

Figure 3d

Flange 4

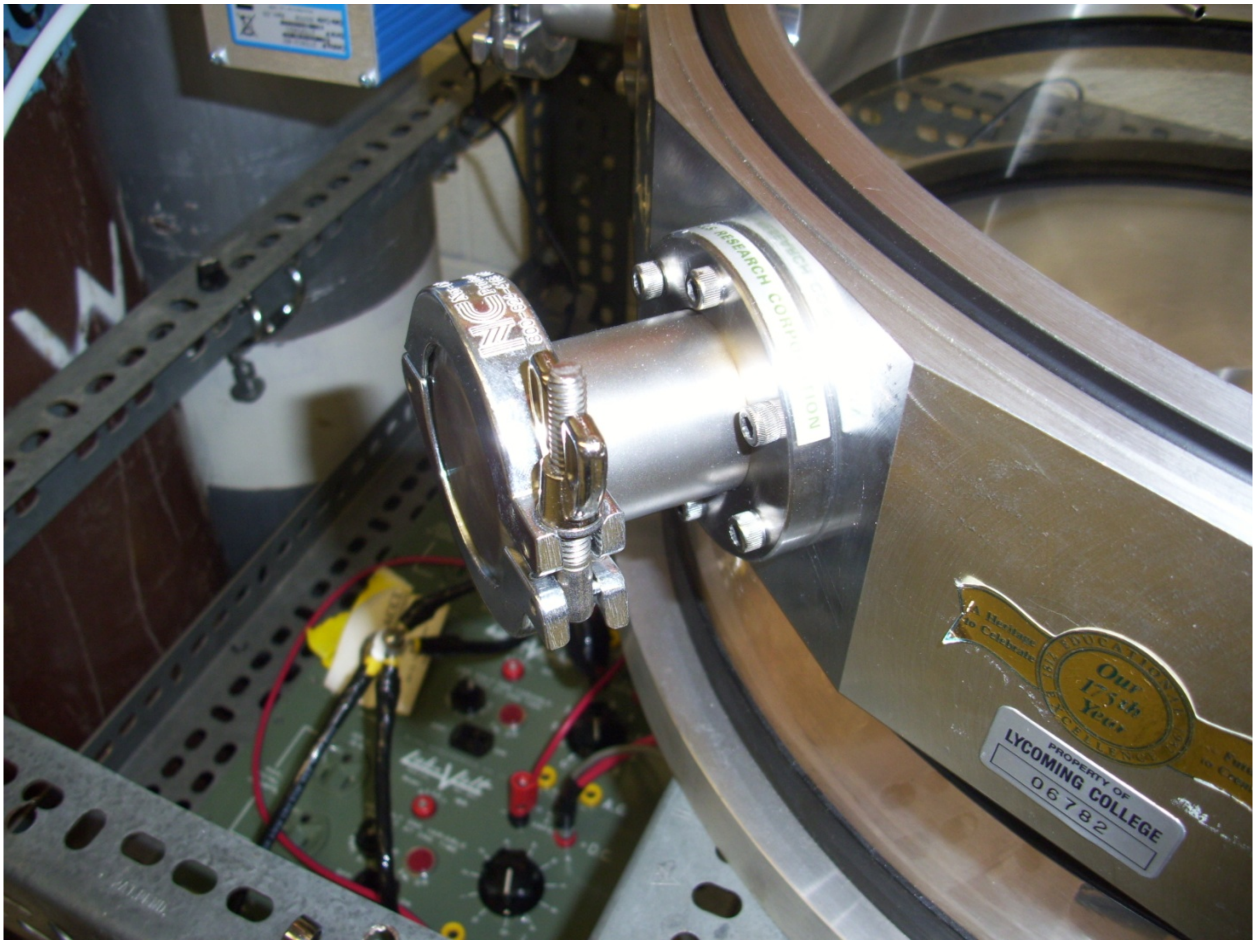

NW-40 blank

Figure 3e

Flange 5

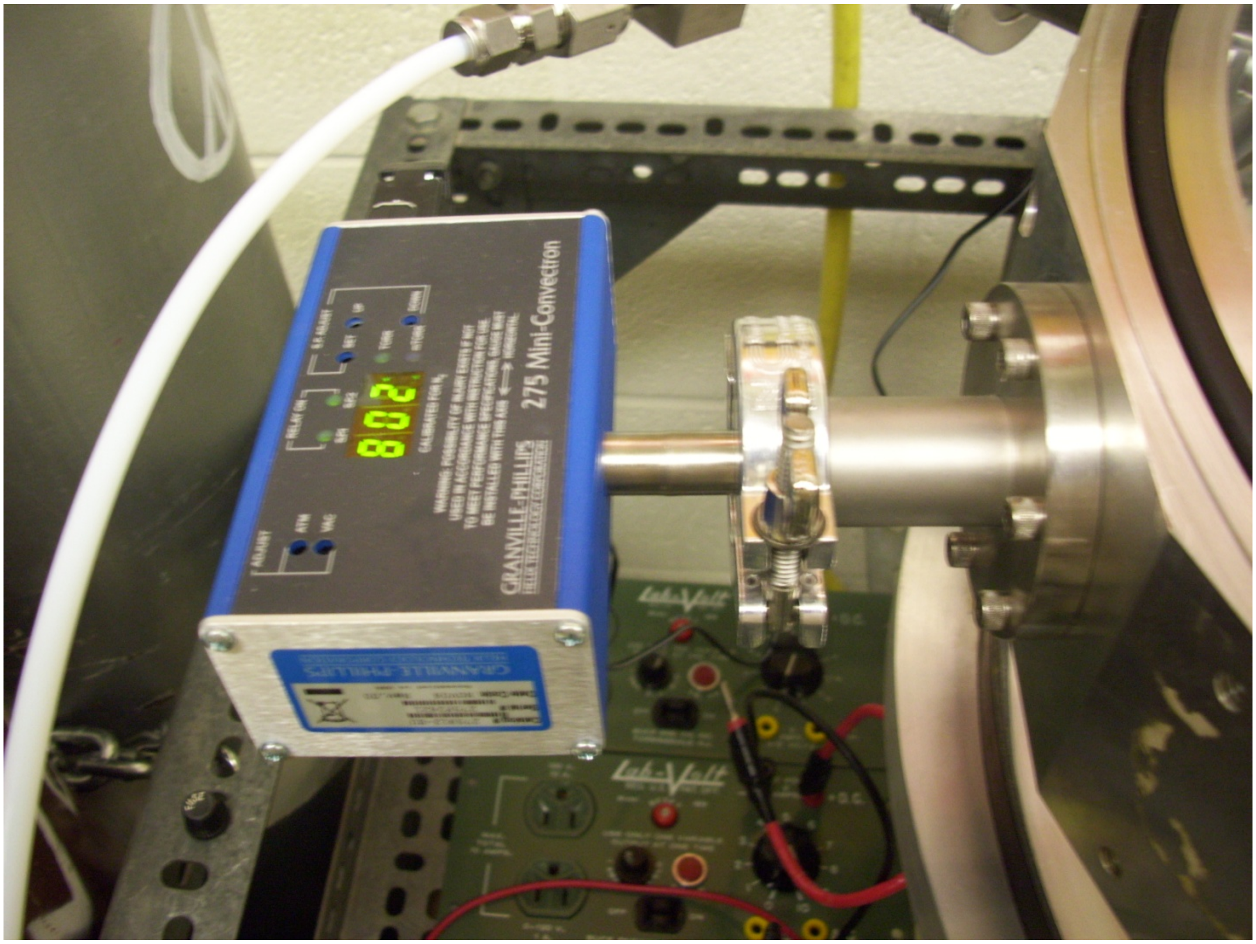

Granville Phillips 275 Mini Convectron

Figure 3f

Flange 6

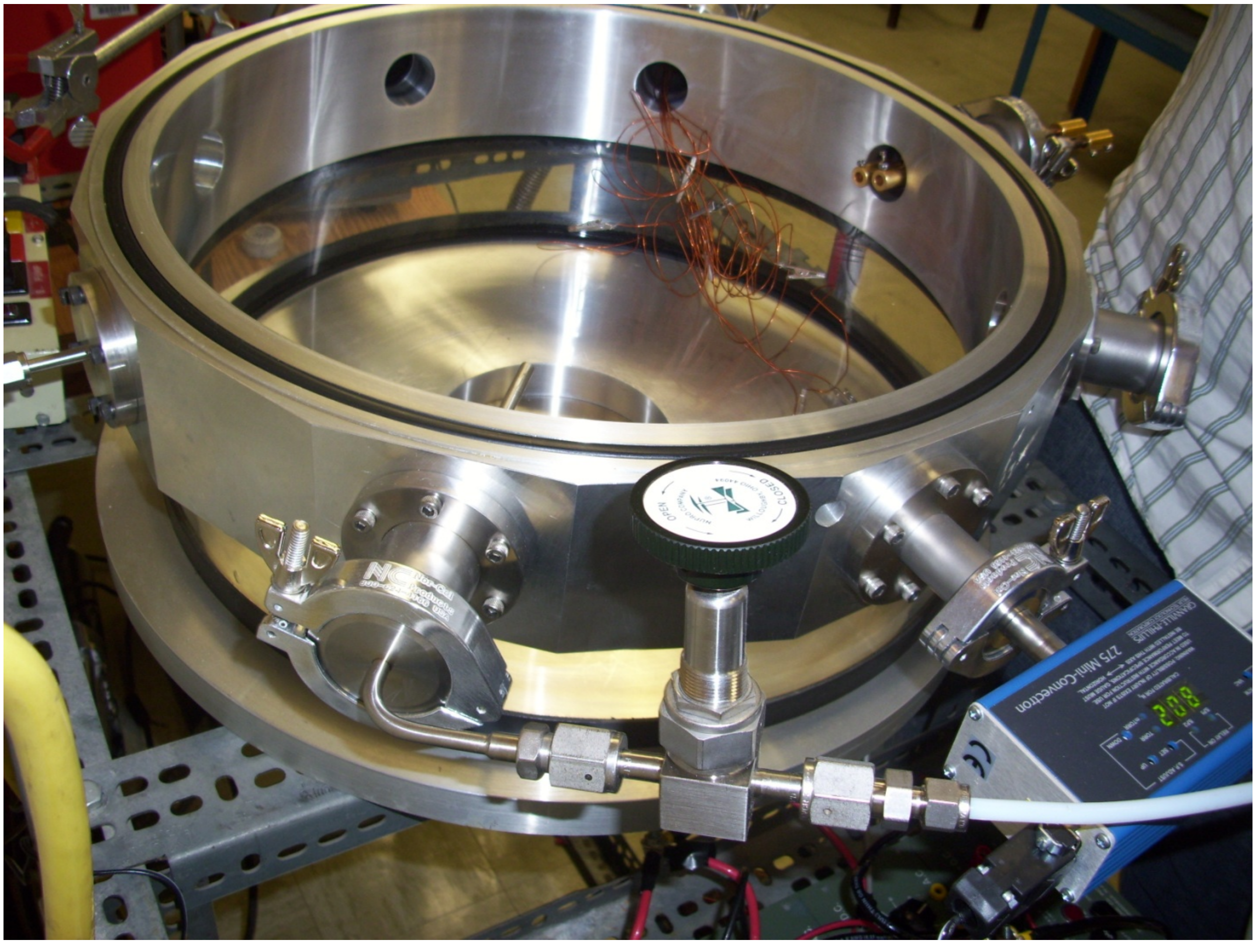

KF NW-40 gas leak

Figure 3g

Flange 7

Swagelok vent

Figure 3h

Flange 8

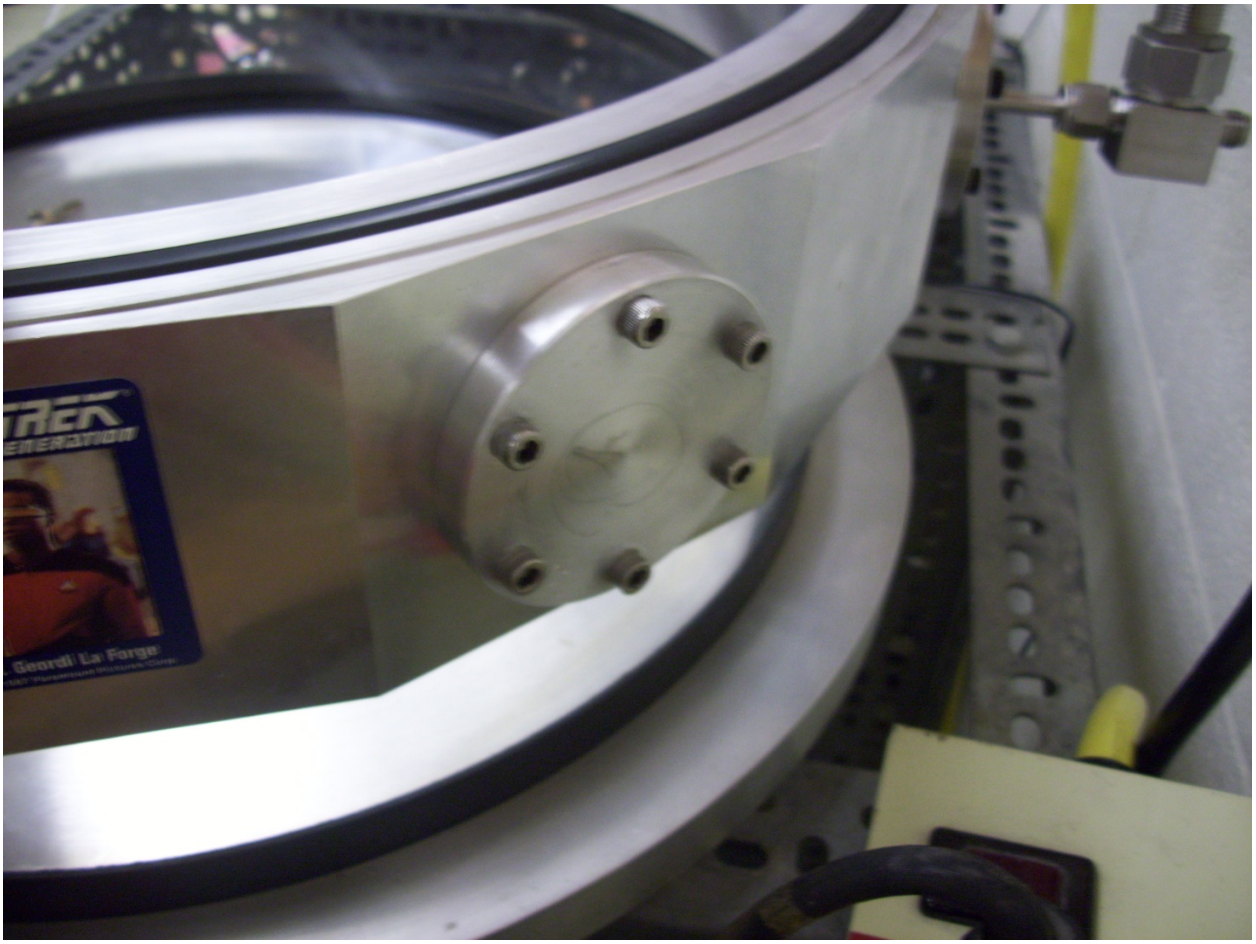

Aluminum blank

Ion Source:

Thermionic emission

One of the first steps to developing an electron theory of metals was made by Paul Drude in 1900.[3] He applied the kinetic theory of gases to an electron gas, and derived the Wiedemann-Franz law which state states that the ratio of the electronic contribution to the thermal conductivity (p) and the electrical conductivity (σ) of a metal.

$$\frac{p}{\sigma} = LT \qquad (2.1)$$

The ratio of $\frac{p}{\sigma}$ is proportional to the temperature (T) and the proportionality constant L, which is known as the Lorenz number.[3]

In 1905 Lorentz applied a Maxwell distribution as the velocity distribution of the electrons inside of the metal.[3] This was a much better statistical method than what was used previously. The newly proposed Drude-Lorentz Theory did not account for Debye's theory of specific heats of solids (2.2).[3]

$$c_v = 9Nk\left[\frac{T}{T_D}\right]^3 \int_0^{\frac{T_D}{T}} \frac{x^4 e^x}{(e^x-1)^2}\,dx \qquad (2.2)$$

Debye's Theory for specific heat of metals did not consider a contribution from the electron gas when in fact a classic electron gas would contribute 3/2 k per electron, where k is the Boltzmann constant, $1.3806503 \times 10^{-23}$ J/K. In 1928, Arnold Johannes Wilhelm Sommerfeld used Fermi-Dirac statistics instead of a Boltzmann statistics to the electron gas.[4]

Assume a constant potential well, A, which is produced by metallic ions. In the well, electrons can move free and independent of other particles. This model proposes a "sea" of electrons relatively free to move in a potential with periodic stationary ionic cores.

Energy level densities for this specific potential well must be derived. The number of levels denoted by dZ which have energies between ε and $\varepsilon + d\varepsilon$ is given by equation (2.3).

$$dZ = 2\pi\left(\frac{2m}{h^2}\right)^{\frac{3}{2}} V\epsilon^{\frac{1}{2}}d\epsilon \qquad (2.3)$$

The mass of an electron is denoted by *m*, and *V* is the volume of the metal. Since electrons have half-integral spin this means they are doubly degenerate and that needs to be accounted for in *dZ*.

Thus,

$$dZ = 4\pi\left(\frac{2m}{h^2}\right)^{\frac{3}{2}} V\epsilon^{\frac{1}{2}}d\epsilon \qquad (2.4)$$

Electrons will occupy the lowest energy level E_0 when the metal is cooled to absolute zero. Evaluating and rearranging equation (2.4), one sees that electrons occupying the lowest possible energy state $E_{0,}$ up to the Fermi energy E_f takes the form of equation (2.5).

$$E_0 = \frac{h^2}{2m}\left(\frac{3N}{8\pi V}\right)^{\frac{2}{3}} \qquad (2.5)$$

This case is represented in Figure (4) where it represents the volume of the shaded region with *N* being the total number of electrons in the system. The work function φ is the energy needed to extract an electron from the metal if it is at the top surface of the metal. Consequently to completely liberate an electron it needs to have energy greater or equal to $E_f + \varphi$. Let this energy value is defined as *A*.

So,

$$E_f + \emptyset = A \qquad (2.6)$$

Refer to figure 4.

Figure 4

Freeing an electron from a potential well in a metal

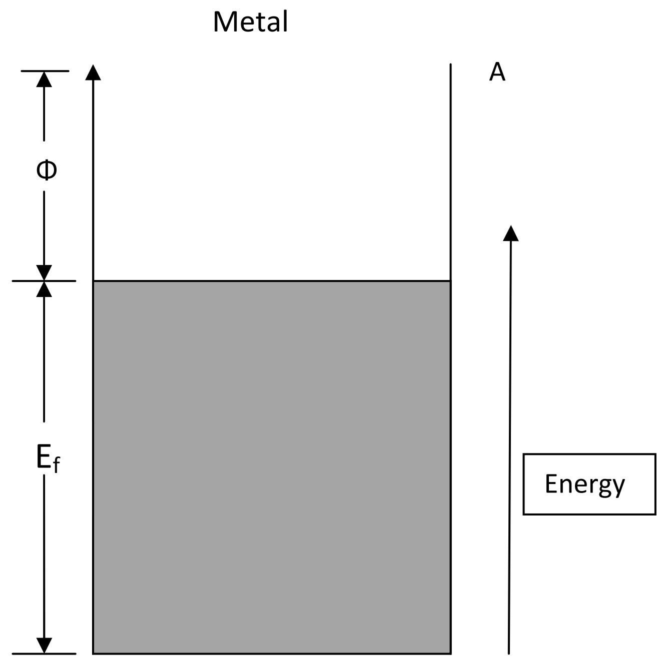

For convenience, at common temperatures, T, the variable B is defined. This is used to show why the Debye theory will not account for total specific heat in metals. B is defined as,

$$B = \frac{2mk}{h^2}\left(\frac{8\pi V}{3N}\right)^{\frac{2}{3}} T \qquad (2.7)$$

The specific heat per electron is found by classical thermodynamics

$$c_v = \left(\frac{\partial E}{\partial T}\right)_v = \frac{\pi^2}{2} kB \qquad (2.8)$$

If one assumes that N/V is 10^{-24} cm^{-3} one can approximate a value of 2×10^{-6} T for B. The specific heat per electron is approximately,

$$c_v = 10^{-5} k\,T \qquad (2.9)$$

The classical value of specific heat is 3/2kT for any monatomic gas.[4]

At temperatures well under the filaments melting temperature there will be a specific amount of electrons liberated from the metal. This is called thermionic emission or the Richardson effect.[4] The strength of this current density, J, can be calculated by using $f(\varepsilon)d\varepsilon$ be the number of electrons per unit volume with energies between ε and $\varepsilon + d\varepsilon$.[5]

$$J = e\int \mathrm{v_x}\, \mathrm{f(\varepsilon)d\varepsilon} \qquad (2.10)$$

The velocity component perpendicular to the surface of the metal is $V_{x,}$ and e is the fundamental charge of the electron 1.602 x 10^{-19} C. The probability for finding electrons with energies between ε and $\varepsilon + d\varepsilon$ is given by the distribution function $f(\varepsilon)$.[5] The Fermi Dirac occupancy factor, $f(\varepsilon)$, is the expectation of a particle having a specific energy of ε.

So

$$J = \frac{2m^3 e}{h^3}\int_A^{\infty}\int_{-\infty}^{\infty}\int_{-\infty}^{\infty}\frac{\mathrm{v_x dv_x dv_y dv_z}}{\mathrm{e^{-v+\mu\varepsilon}+1}} \qquad (2.11)$$

where the variable μ is defined as

$$\mu = \frac{1}{kT} \qquad (2.11)$$

The limits of integrations for the y and z components run from -∞ to ∞. The limits for the X component integration ran from A to ∞ because only those electrons that possess a sufficient amount of energy can be liberated from the metal.

Using the relationship,

$$\mathrm{v_x} = \frac{1}{m}\frac{\partial \epsilon}{\partial \mathrm{v_x}} \tag{2.13}$$

Obtained from the definition of kinetic energy, the current density then takes the form,

$$J = \frac{2m^3 e}{h^3}\int_{-\infty}^{\infty} dv_y \int_{-\infty}^{\infty} dv_z \int_{\varsigma}^{\infty} \frac{d\epsilon}{1+\mathrm{e}^{-\nu+\mu\varepsilon}} \tag{2.14}$$

where,

$$\varsigma = A + \frac{1}{2}m({v_y}^2 + {v_z}^2) \tag{2.15}$$

Integrating over ε the resulting equation becomes

$$J = \frac{2m^3 e}{\mu h^3}\int_{-\infty}^{\infty} dv_y \int_{-\infty}^{\infty} dv_z\, ln\left[1 + e^{v-\mu\left(A+\frac{1}{2}m({v_y}^2+{v_z}^2)\right)}\right] \tag{2.16}$$

At ordinary temperatures, T, the exponential is small compared to one, and a series expansion for the logarithm can be used such that,

$$J = \frac{2m^3 e}{\mu h^3}\int_{-\infty}^{\infty} dv_y \int_{-\infty}^{\infty} dv_z e^{v-\mu\left(A+\frac{1}{2}m({v_y}^2+{v_z}^2)\right)} \tag{2.17}$$

or

$$J = \frac{4\pi m e}{\mu^2 h^3} e^{v-\mu A} \tag{2.18}$$

As long as temperatures are "reasonable" equation (2.17) takes the form of the Richardson equation.

$$J = \frac{4\pi me}{h^3}\, k^2 T^2 e^{-\frac{\phi}{kT}} \tag{2.19}$$

Testing for thermionic emission

A beam line can be obtained from the ion production by placing the region that is creating ions near an electric field. The electric field will either attract or repel ions based on the polarity of their charge. Positive ions will move in the direction of the field, while negative ions will move in the opposite direction of the field. These ions can be directed by using different focusing techniques.

If a circular metal washer is placed near a region of ions, the symmetry of the electric field will focus the ions into a beam with a particular velocity. Once the ions are traveling in a beam they can be directed to bombard a grounded plate. Electrical potential will build up on the plate and cause a current to flow to the ground. This current when measured provides show evidence for ion production by means of thermionic emission.

Direct ionization from an electric field

When an atom is placed in a sufficient electric field at proper pressure it will ionize. The electrons will be liberated from the atom and it will move in the opposite direction of the electric field, what is left is a positively charged ion which will then move in the direction of the electric field. The amount of energy required to liberate electrons from an atom is called the ionization energy. Ion production by this means is a possibility for future work pending the outcome of thermionic emission ion production.

Magnetic and Electric Field System:

Solenoids

A long straight coil of wire can be used to generate a nearly uniform magnetic field similar to that of a bar magnet. The magnetic fields arise from Ampere's law.[6] (Refer to figure 5)

$$\oint B \cdot dl = \mu_0 I_{enclosed} \tag{3.1}$$

Figure 5

Ampere's Law when using solenoids

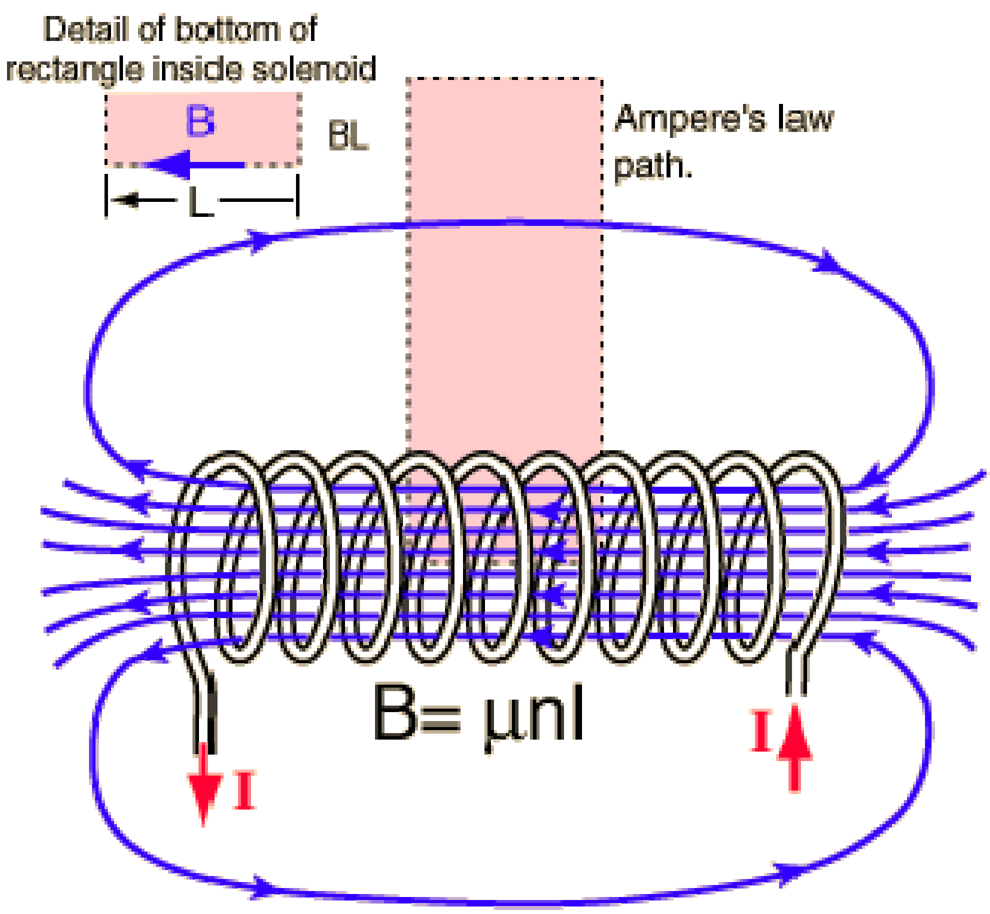

* http://hyperphysics.phy-astr.gsu.edu/hbase/magnetic/solenoid.html

Equation (3.1) is the general form of Ampere’s law. The form that is commonly used when dealing with solenoids is,

$$BL = \mu_0 NI \qquad (3.2)$$

where, *B* is the magnetic field, *L* is the length of the coils, μ_0 is the absolute permeability of free space 4π X 10^{-7} T·m·A^{-1}, N is the number of turns of coil, I is the current flowing through the coils.[6] Then after calculating the resistance of the wire used in the coils of the solenoid, Ohm’s Law is used to introduce voltage into equation (3.2)

$$V = IR \qquad (3.3)$$

Calculating the magnetic field produced by a solenoid at a particular voltage for the equation one sees,

$$Bl = \frac{\mu_0 NV}{R} \qquad (3.4)$$

A first attempt in producing a uniform magnetic field for a cyclotron was to encompass the dee’s inside a hollow core solenoid. A hollow core solenoid was constructed out of 14 gauge copper wire, with *N* being 600. The idea of a hollow core solenoid was abandoned after testing the uniformity and strength of the magnetic field that was produced because the field strength was to weak while the coil was turned on to full current allowance through the wire.

The next approach was to use two metal core solenoids which both had a resistance of 62.5Ω, and have the dees placed between the solenoids. Since many metals have high magnetic susceptibility, iron was placed at the core of a solenoid to produce a larger magnetic field. The new design would allow for two separate solenoids which individually had a total of 3,400 turns of wire, thus producing a greater more uniformed magnetic field of greater strength.

Calculating the permeability of a metal core solenoid

Metal core solenoids follow a form of Ampere's law, which linearly relates magnetic field to the amount of current passing through the coils.

$$BL = \mu_k N I \qquad (3.2)$$

where

$$\mu_k = \alpha \mu_0 \qquad (3.5)$$

Putting equation (3.2) and (3.5) in the form

$$B = \left\{\frac{\alpha \mu_0 N}{L}\right\} I \qquad (3.6)$$

One can see there is a distinct linear relation of the magnetic field to the current flowing through the coils.

Using a PASCO Xplorer GLS unit the average magnetic field was systematically mapped out over the surface face of the solenoid with different settings of current flowing through the coils. The sensor has a resolution of 0.01 Gauss at 10 Hz. (Refer to Figure 6) Assuming that y=B, x=I we can neglect the intercept term and then determine the slope to calculate α.

See Figure 6.

Figure 6

Magnetic Field Strength as a Function of Current

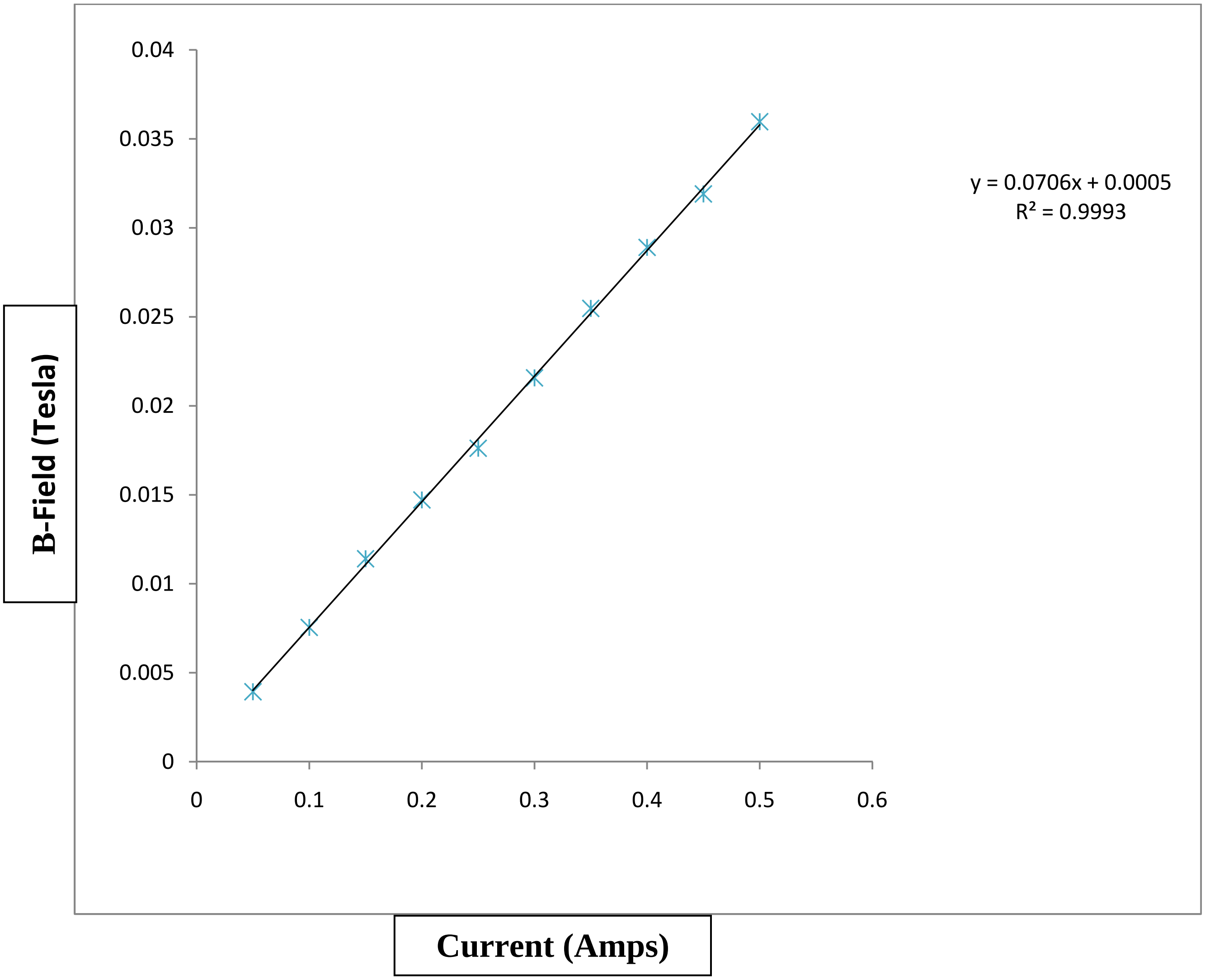

Data Calculations for a Metal Core Solenoid

From this data the slope was found to be 0.0706. This was then equated to the bracketed term in equation (3.6)

where, $$0.0706 = \left\{\frac{\alpha\mu_0 N}{L}\right\} \qquad (3.7a)$$

$$\frac{0.0706(L)}{\mu_0 N} = \alpha \qquad (3.7b)$$

With, L= 0.1m, N=3400 turns, μ_0= $4\pi \times 10^{-7}$ T·A·m^{-1}, one calculates $\alpha = 30.16$

With that value of alpha, it is possible to obtain approximately a 1 Tesla field by supplying the solenoids with sustainable amounts of current. A lower current flowing through the wire there will involve less power being drawn into the system, and a lesser chance for the wires to melt and cause a short which in turn would damage the entire solenoid. There is more possibility for contamination from outgassing of the wires if they are greatly heated as well. Also vacuum stability and low pressures are compromised with large thermal gradients inside and around the chamber.

Detection System:

The detection system is designed to be mobile. It is an aluminum L-shaped plate with dimensions 83mm by 53mm and the plate is 1.5 mm thick. The bottom of the plate is wrapped in Teflon tape to insulate and prevent any discharge to the bottom of the chamber.

The plate was the connected to one of the pins on the 8-pin electric feedthrough. The outside corresponding pin was then connected to a micro ammeter which was then connected to ground.

This circuit allowed for a detection of charged particles in the vacuum. If a beam of charged particles hit the plate it will produce a potential on the surface of the plate. Being that the circuit is connected to ground the high potential will cause a current to flow through the wire. By this means charged particles and beams can be proven to exist inside the chamber.

Plate Detection Circuit:

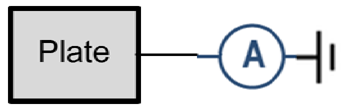

Test Procedure and Results:

<u>Outgassing Test of Hardware</u>

Materials that are subject to high vacuum experience outgassing. Outgassing is when adsorbed matter is ejected from a material surface. The ejected matter can cause contamination and a weaker vacuum. Each piece of hardware was tested independently to calculate the chambers pump down rates.

The magnetic system has the greatest outgassing rate. The data shows that after 20 minutes of pumping with the magnets in the chamber the pressure was 0.555 Torr. After 20 minutes of pumping with an empty chamber the pressure was 0.052 Torr. Hence obtaining desired pressures will take substantially longer with the magnets inside of the vacuum environment. Refer to Figure 7

The materials were then tested with a full liquid Nitrogen (LN2) trap. This dramatically increased the pressure pump down rates with the greatest influence being on the magnets. With the magnets in the chamber and the LN2 trap in use the pressure reached 39 mTorr range within 9 minutes as opposed to without the LN2 trap which took 60 minutes. Refer to Figure 8

Figure 7

Vacuum Chamber Pump down rates

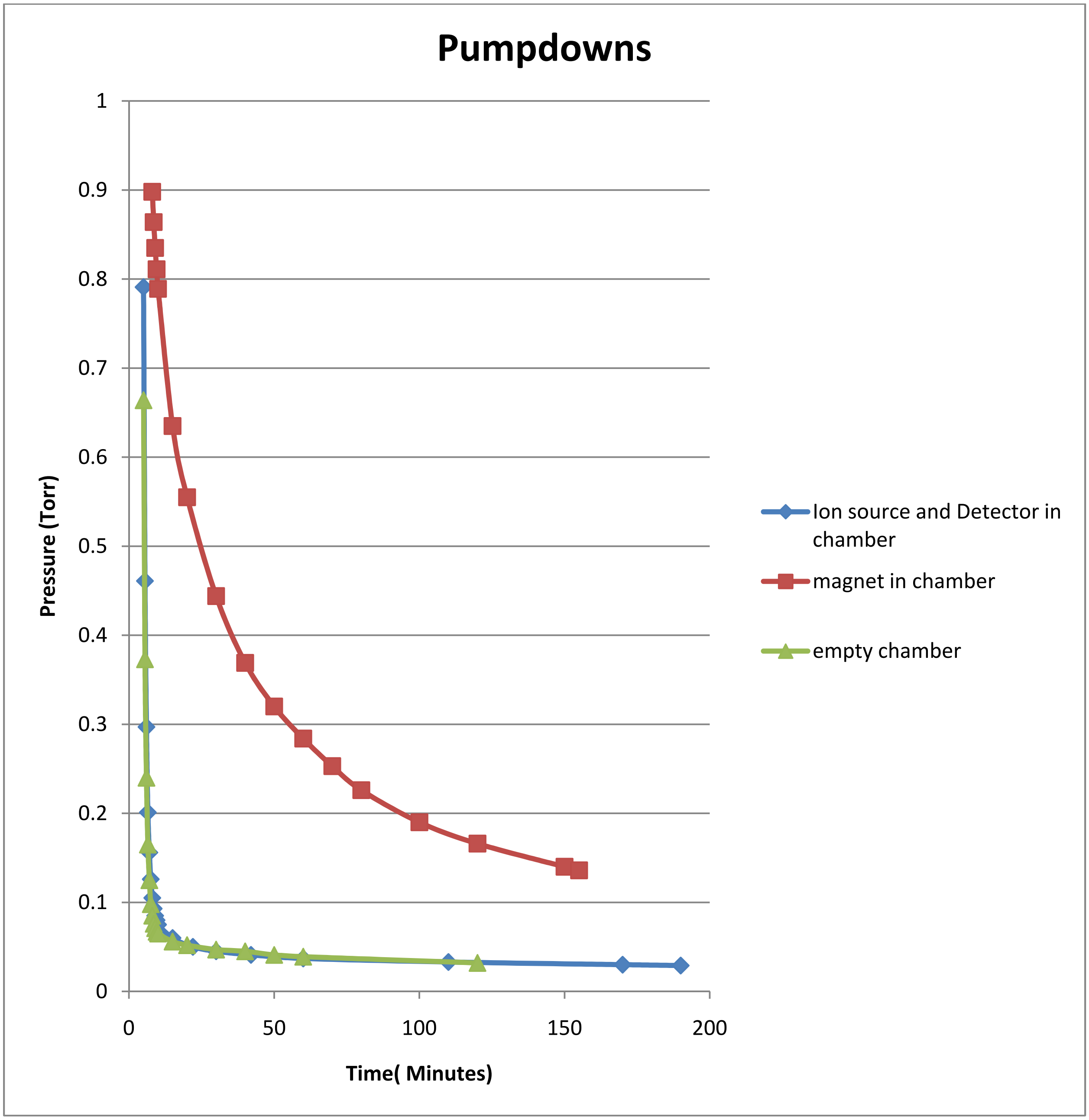

Figure 8

Vacuum Chamber Pump down rates with LN2 trap in use

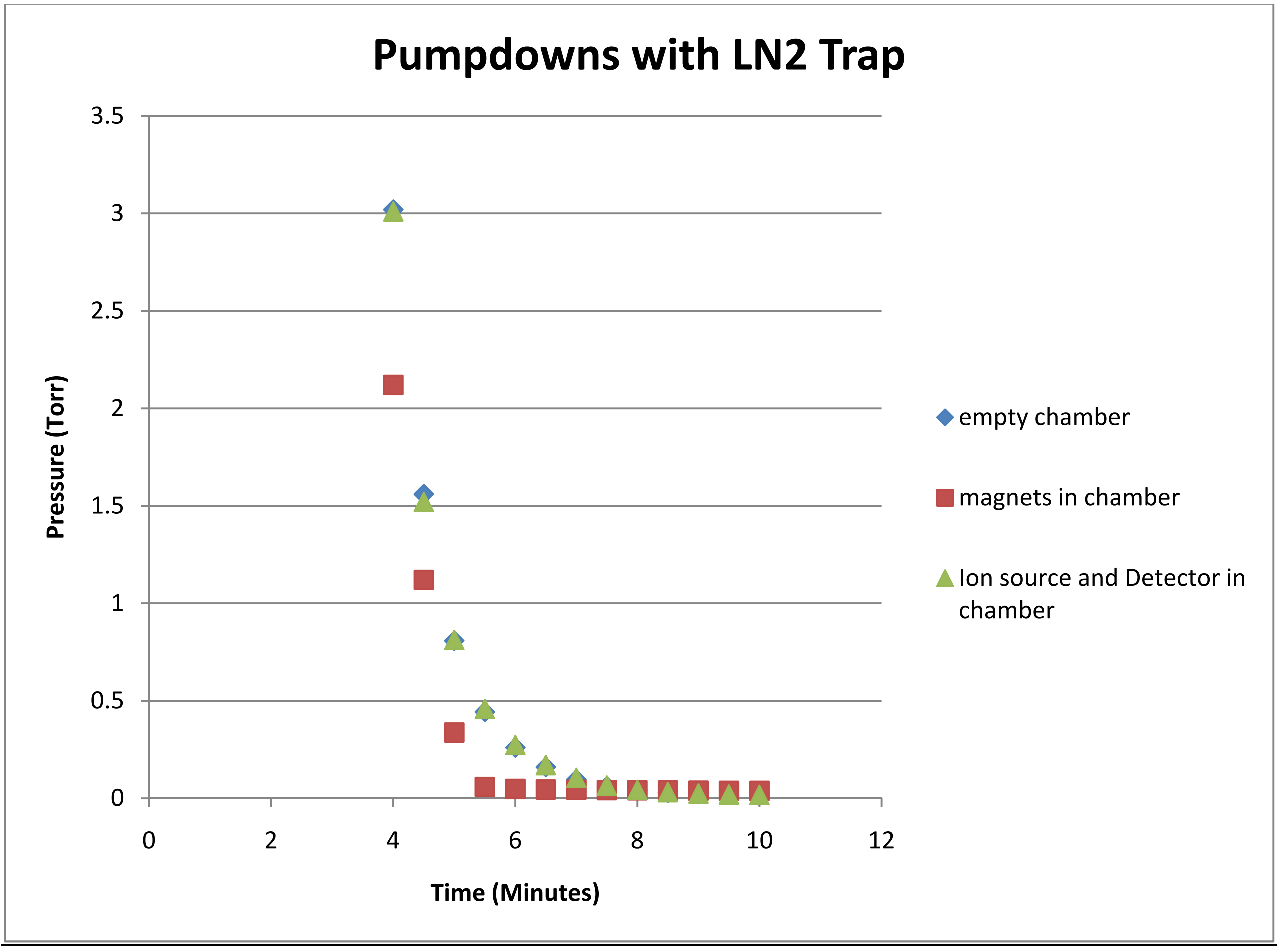

Testing Filaments

The filaments used were Tungsten wire filaments taken from the inside of light bulbs having a diameter of 0.127mm. A standard light bulb fixture made for an easy case to mount the filament. The filament was then heated by a 130V variable AC source and had a white light glow from the filament. The detector plate was placed at specific locations to obtain data.

Testing the Richardson Equation:

The detector plate was place perpendicular to the filament strip at a distance of 4 cm. The chamber pressure was dropped to 41-42 mTorr and the filament was heated by increasing the voltage from the AC variable power supply. The voltage was increased in 5 volt increments and current from the detector plate was measured.

Voltage (V)	Detector Current (μAmps)
55	1
60	2
65	4
70	8
75	12
80	21
85	25
90	48
95	71

The data was then fit to an equation that mimicked the form of the Richardson equation.

$$J = Ax^2e^{-B/x}$$

Refer to figure 9

Figure 9

Detector Plate Current vs. Voltage

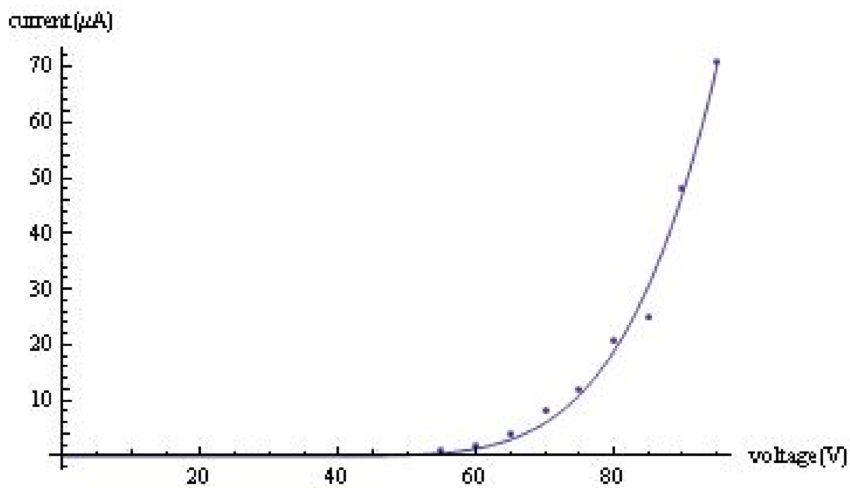

$$J = Ax^2 e^{-B/x}$$

A = 1.41 and B = 494.109

$R^2 = 0.923$

*Method of finding level of fit

$$R^2 = 1 - \frac{\sum_{i=1}^{n} (Y_{(fit)i} - Y_{(obs)i})^2}{\sum_{i=1}^{n} (Y_{(obs)i} - \bar{Y}_{obs})^2}$$

Testing the Filament Emission Field

The emission current was recorded at various positions on the surfaces of concentric spheres with different radii. The center dot represents the filament and the dots on the surface of the sphere represent the plate positions.

See Figure 10.

Figure 10

Plate Locations

= Plate measurements

= Filament

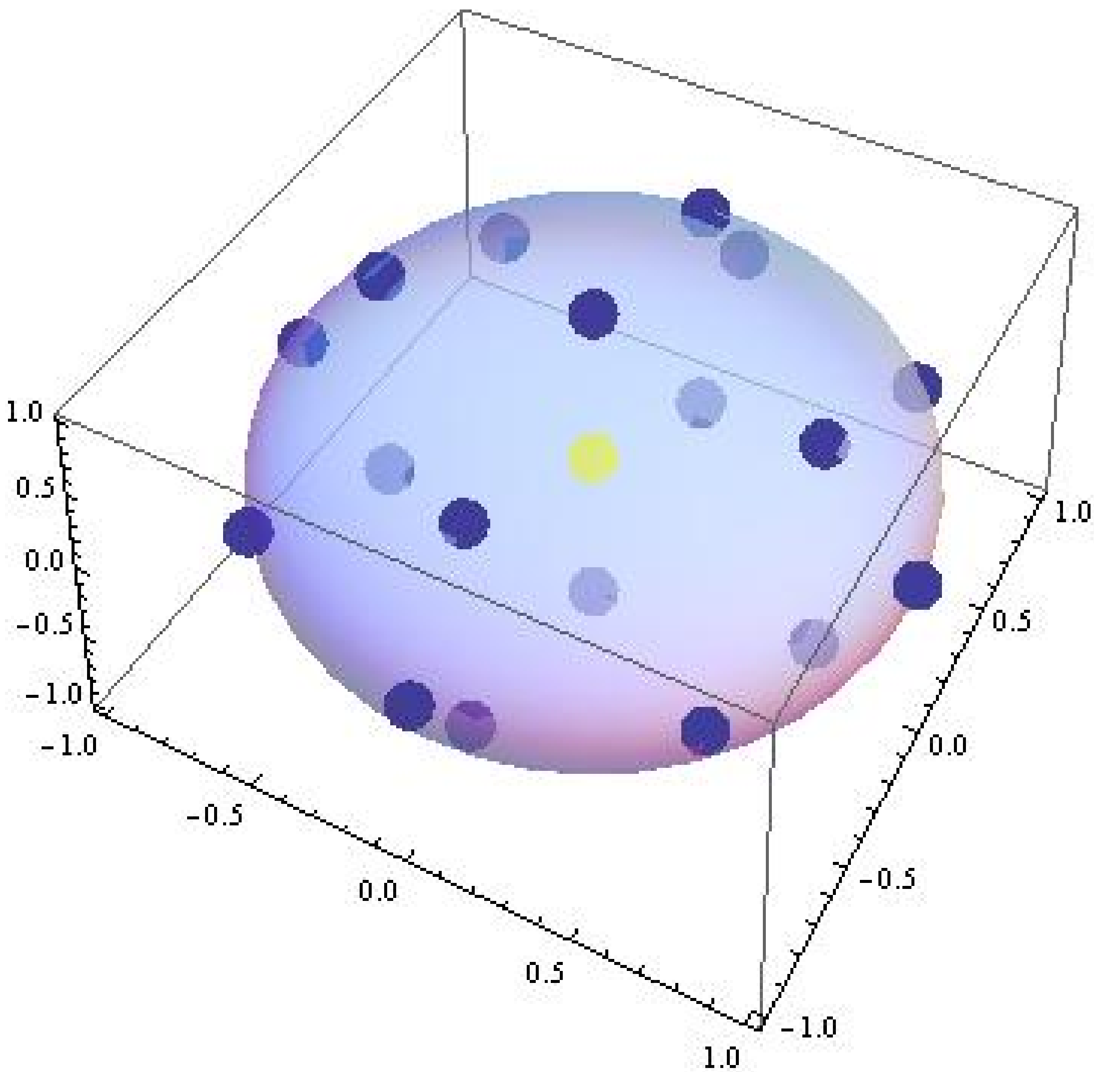

Table 1.

Chamber Pressure: 45 mTorr

Filament voltage: 75V AC

Position	r =2cm	r =3cm	r =4cm	r =5cm	r =6cm
(Φ,θ)	Current μA	Current μA	Current μA	Current μA	Current μA
180,0	36	22	15	8	6
180,45	36	22	14	8	7
180,-45	35	21	13	10	6
135,0	36	22	14	9	7
225,0	35	23	15	9	7
0,90	34	22	15	10	8
0,-90	34	21	14	9	6
90,45	33	22	15	9	7
90,0	35	23	14	10	7
90,-45	35	23	14	8	7
270,0	35	20	14	10	6
270,-45	34	22	14	9	7
270,45	34	21	13	8	6
0,45	30	16	9	4	1
45,0	36	22	15	8	6
315,0	34	21	13	8	6
0,0	30	16	9	4	1
Mean	34.222222	21.333333	13.555556	8.6111111	6.1111111

Table 2.

Chamber Pressure: Unknown, (<1mTorr)

* Granville Phillips 275 Mini Convectron cannot read below 1mTorr. An ion gauge would be required to obtain an accurate pressure.

Filament voltage: 75V AC

Position (Φ,θ)	*r* =2cm Current μA	*r* =3cm Current μA	*r* =4cm Current μA	*r* =5cm Current μA	*r* =6cm Current μA
180,0	63	39	24	15	12
180,45	65	40	26	16	13
180,-45	66	41	27	18	14
135,0	67	43	27	17	15
225,0	65	42	26	19	13
0,90	67	42	28	19	15
0,-90	67	43	28	18	14
90,45	66	41	27	19	14
90,0	65	42	27	18	15
90,-45	66	42	29	20	14
270,0	67	41	28	18	15
270,-45	66	41	27	19	14
270,45	65	42	28	19	13
0,45	67	42	26	18	15
45,0	65	41	28	17	14
0,-45	65	41	27	17	13
315,0	66	41	26	18	15
0,0	56	35	20	12	8
Mean	65.222222	41.055556	26.611111	17.611111	13.666667

Figure 11

Average Current vs. Distance from Source

The plate detector current is lower when the pressure is higher in the chamber. This is because of the amount of electrons that bombard the plate are less, at higher pressures the electrons are more likely to interact with molecules in the chamber and possibly lose energy. At lower pressures the electrons can flow with less interference of gas molecules. Refer to Figure 12.

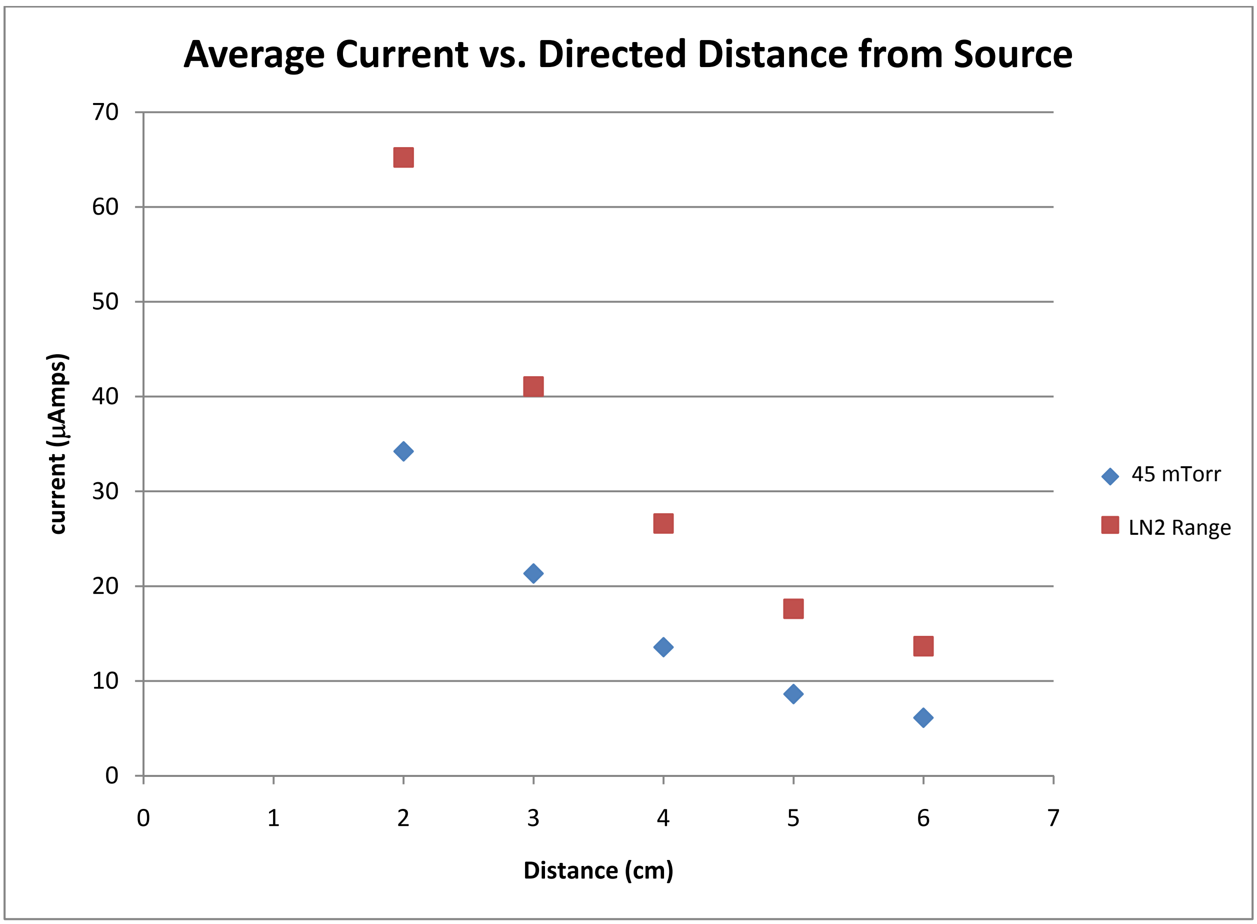

Figure 12

Density Plot of Emission (45 mTorr)

Cross section of the filament in the x-y plane depicting the density of electrons in that plane

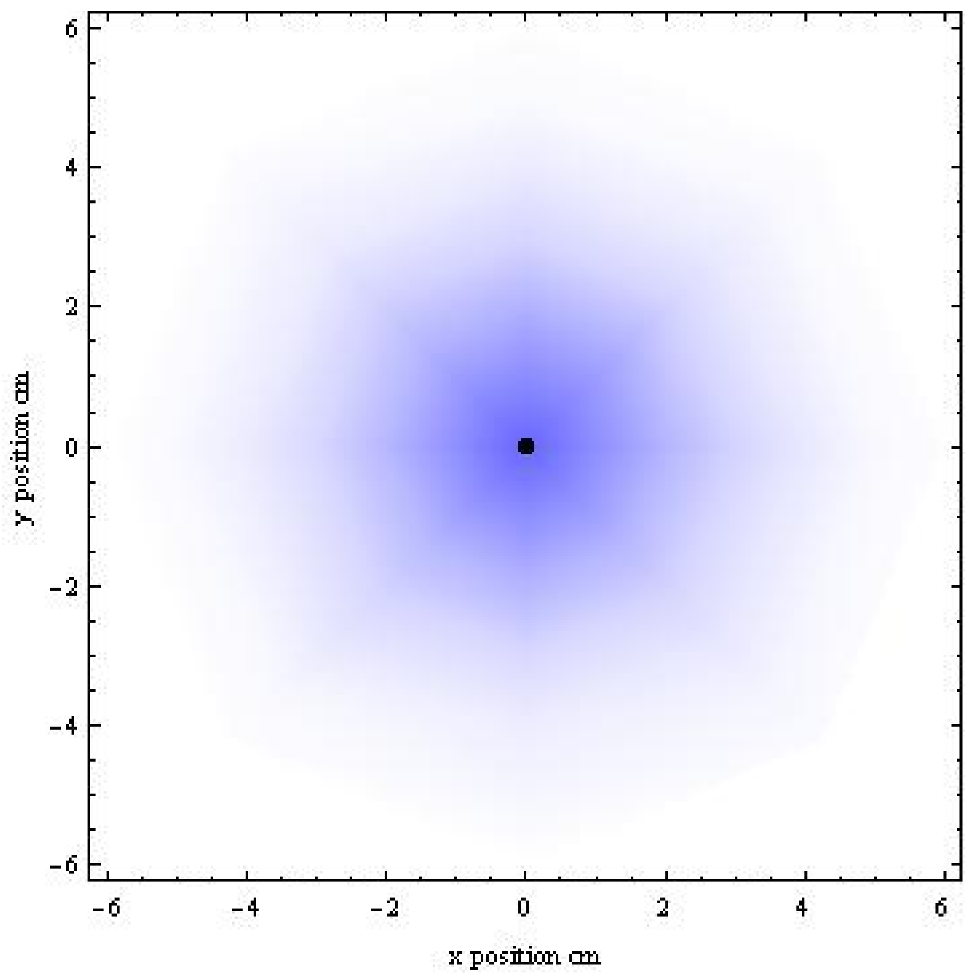

For: Chamber Pressure: 45 mTorr

Filament voltage: 75V AC

Figure 13

Density Plot of Emission (LN2 Range)

Cross section of the filament in the x-y plane depicting the density of electrons in that plane

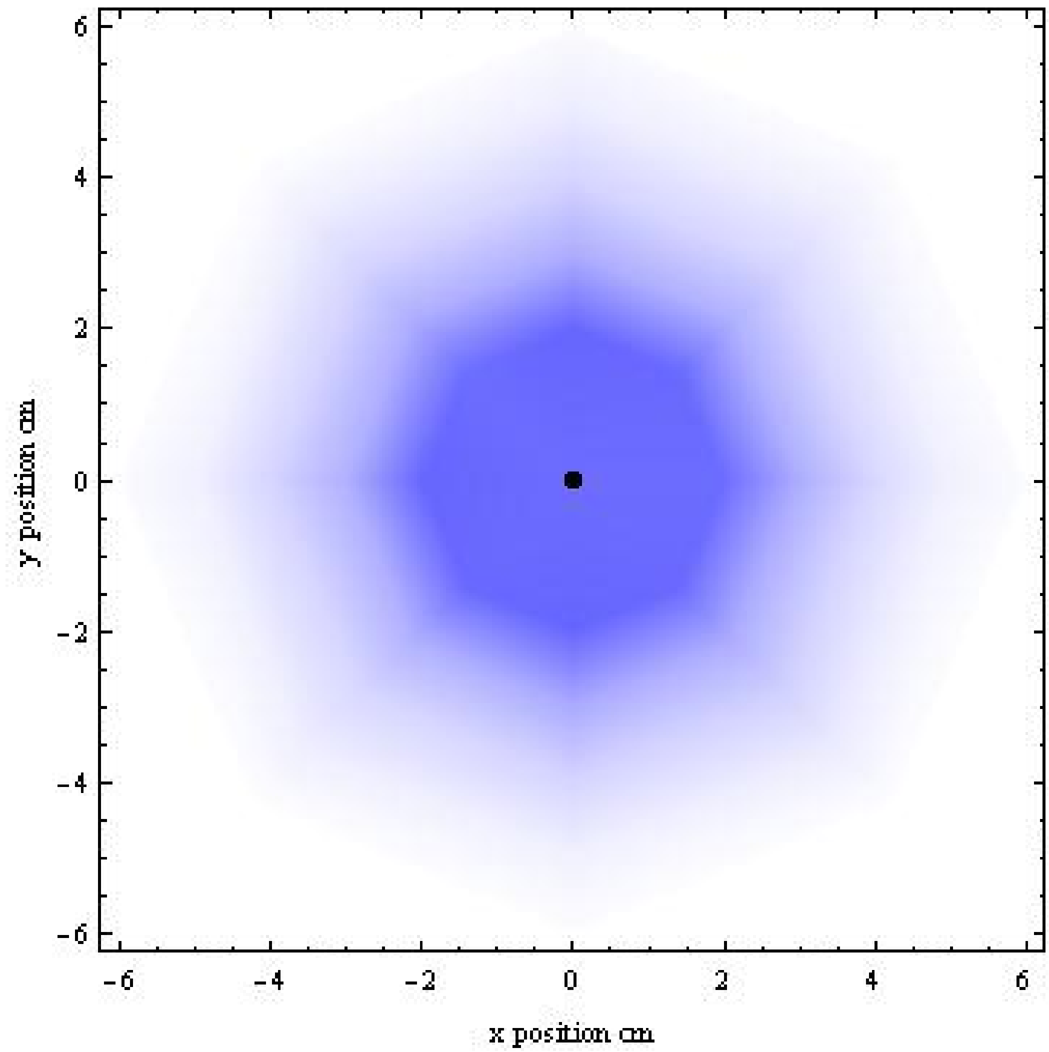

For: Chamber Pressure: LN2 Range

Filament voltage: 75V AC

Testing the Accelerator Grid

The filament was then tested with an accelerating grid. The gird had a 2KV potential over it and was placed 2.5 cm from the filament source the grid focused the electron beam to have a cross-sectional area of 28.274 mm^2. The detector plate was placed a distance of 5 cm from the filament source.

Figure 14

Detector Plate Current vs. Voltage

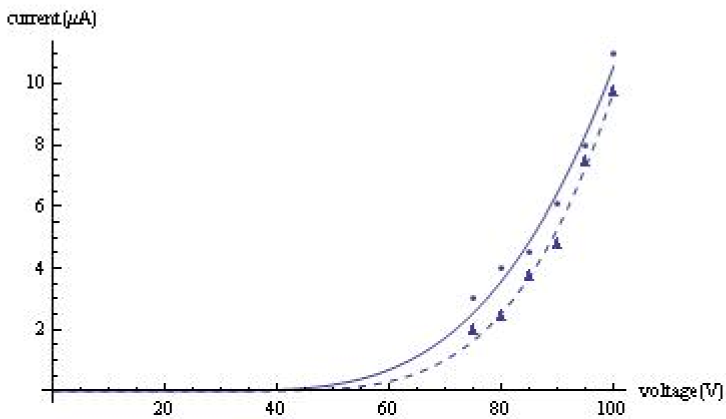

$$J = Ax^2 e^{\frac{-B}{x}}$$

No Field =

A= 0.0358and B= 360.461

*R^2 = 0.954

2KV Field =

A= 0.0133 and B=253.298

*R^2 = 0.892

*Method to finding level of fit

$$R^2 = 1 - \frac{\sum_{i=1}^{n}(Y_{(fit)i} - Y_{(obs)i})^2}{\sum_{i=1}^{n}(Y_{(obs)i} - \bar{Y}_{obs})^2}$$

Discussion:

The Lycoming College vacuum chamber originally belonged to a former physics professor Dr. Morton Fineman. He used the chamber for molecular beam experiments in inert gases. After Dr. Fineman retired, Dr. David G. Fisher used the vacuum chamber to house metal samples which he had produced in his graduate school research. The vacuum chamber was a perfect place to store his materials because it produced a very safe and clean environment.

In the fall of 2006, alumnus Ms. Melany McGillvary ('07) took on the task of refurbishing the chamber. Melany was able to adapt the chamber to a pressure of about 147 mTorr. She received much help and many donations from alumnus Mr. Jeff Garrett ('81).

After the chambers most recent upgrade from the fall of 2008- 2009, the lowest recordable pressure is 1mTorr which could not have been possible without the previous work of Ms. McGillvary. The chamber pressure does go below 1mTorr, but the type of gauge currently in use only allows for pressure measurement ranging from 900 Torr to 1 mTorr. This extra pressure drop is due to new addition of the LN2 trap. The trap, donated by Mr. Jeff Garrett, was tested at OSI (Outgassing Services International) lab where it was outfitted to a state of the art outgassing chamber. The trap was connected to a larger chamber in a similar fashion to the way it is currently being used here at Lycoming and the recorded pressure at OSI was 5×10^5 Torr. It is reasonable to postulate that when the LN2 trap is in use with the Lycoming chamber it is near the same pressure range. The chamber is now moderately adapted to work and do experiments.

A wide range of tests have been conducted to understand the capabilities of the current chamber, study charged particle dynamics, and construct a platform for a plethora of experiment that can now be performed. One of the original goals, the building of a cyclotron, could not have been reached due to budget restrictions. A cyclotron is practically 90% complete. An RF amplifier is needed to strengthen the potential on the dees of the cyclotron. The chamber now has the capability to obtain an electron beam, which is a great asset for the chamber and has allowed for many current and future experiments to be conducted.

Works cited

1. Lawrence, Ernest O., and Stanley M. Livingston. "The Production of High Speed Light Ions without the Use of High Voltages." *Physical Review* 40.1 (1932). Print
2. Coughlan, G. D., J. E. Dodd, and B. M. Gripaios. The Ideas of Particle Physics : An Introduction for Scientists. New York: Cambridge UP, 2006.
3. Harr, Ter. Elements of Statistical Mechanics. United States Of America, 1954.
4. Schroeder, Daniel. An Introduction to Thermal Physics. 25 Aug. 2005. 27 May 2009
5. McQuarrie, Donald. Statstical Mechanics. University Science Books; 2 edition (May 2000)
6. Halliday, David. Resnick Robert. Walker Jearl. Fundamentals of Physics. 7th Ed. Wiley; 7 edition (June 14, 2004)
7. M.L.McGillvray. Analysis of Internal Vacuum Chamber Pressure Efficiency. (2006)
8. - Close, Frank. Particle Physics. New York: Oxford UP, Incorporated, 2004.
9. -Hill, Robert D. Tracking Down Particles. New York, NY: W.A. Benjamin, Inc, 1963.
10. -Wilson, E. J. An Introduction to Particle Accelerators. New York: Oxford UP, 2001.

Additional readings

a. A Chambers, R.K. Fitch, B.S. Halliday. Basic Vacuum Technology. (1998)
b. LAFFERTY; JAMES. Foundations of Vacuum Science and Technology. New York : J. Wiley & Sons, 1997.
c. D.M. Hata. Introduction to Vacuum Technolohy. (2007)
d. White, Harvey, Elliott**.** Modern college physics New York, Van Nostrand Reinhold Co. (1972)
e. Walecka, John Dirk.Introduction to modern physics : theoretical foundations. New Jersey : World Scientific, (2008)
f. Melissinos, Adrian C.. Experiments in modern physics. New York, Academic Press (1966)
g. William D. Bygrave, Paul A. Treado, James M. Lambert. Accelerator nuclear physics; fundamental experiments with a Van De Graaff accelerator. Burlington, Mass., High Voltage Engineering Corp. (1970)
h. Sard, R. D. Relativistic mechanics; special relativity and classical particle dynamics. New York, W. A. Benjamin, 1970
i. Richard, Patrick. Atomic physics, accelerators. New York : Academic Press, (1980)
j. Kittel, Charles. Elementary statistical physics. New York, Wiley (1958)
k. Kelly, Don C. Thermodynamics and statistical physics; an elementary treatment with contemporary applications. New York, Academic Press (1973)

Acknowledgements

- Dr. David G. Fisher, Physics (Advisor, Honors Committee)
- Dr. Christopher W. Kulp, Physics (Honors Committee)
- Dr. Gene D. Sprechini, Mathematical Sciences (Honors Committee)
- Dr. Jeremy D. Ramsey, Chemistry (Honors Committee)
- Dr. Richard Erickson, Astronomy
- Provost Thomas Griffiths, Ph.D.
- Mr. Jeff Garrett, Class of 1981
- Lycoming College Chemistry Department
- Melanie Taormina, Director of Alumni Relations, Class of 1994
- Melany McGillvray, Class of 2007
- Miss Jenn Campbell, Lab Instructor, Class of 2002
- Lycoming College Buildings and Grounds
- Lycoming College Night Cleaning Staff
- Family

Setting up an Electron Beam in the Lycoming College Vacuum Chamber

This manual explains step by step how to produce an electron beam. It discusses setting up the filament, chamber, detector plate, and electric field.

Preparing the Filament

The filaments are made of tungsten wire taken from the inside of standard light bulbs. A fully functional light bulb is cracked at its glass base of the glass using a file. This will allow for the bulb to break its vacuum seal and not shatter the glass. The glass blub is then removed, exposing the metal and glass base that holds the filament. Note: Be careful not to bend or break the filament.

Preparing the Casing for the Beam

The beam casing is a rectangular Plexiglas box which has posts to which the accelerator grids are mounted. Take the filament and screw it into the light bulb fixture which is mounted at the back end of the beam casing. Again take special care of the filament and do not bend or touch with bare hands. Next the accelerator grids are attached to the posts of the beam casing. These can be either mesh grids or aluminum foil. The mesh grids accelerate electrons in a field producing more of a group of accelerated electrons as opposed to a beam. Using aluminum foil will produce a better representation of a beam. A piece of flat aluminum foil with a small pin hole is attached to the posts. There are currently two posts for two separate accelerator grids which allows for different positions and use of multiple accelerating grids.

Preparing the Chamber

The beam casing is carefully placed into the chamber. The filament is the connected with two of the wires from the 8-pin feedthrough in the chamber. These pins on the outside of the chamber are connected to a variable AC source (Variac Transformer Model Number TDGC-2KM). The accelerator grid is then connected with a wire from the 8-pin feedthrough in the chamber. The corresponding pin outside of the chamber is then connected to the positive terminal of an HV power supply (Griffin 5kV EHT Supply), the negative terminal is connected to one of the wires that connect the filament. The detector plate, an aluminum L-shaped plate, is placed in the chamber in whatever area is being investigated. The detector plate is then connected to a wire from the 8-pin feedthrough in the chamber. The corresponding pin that is outside the chamber is then connected in series to a micro-ammeter and then to ground. This will allow any potential that is produced on the plate to cause a current to flow through the wire which can be measured.

Turning on the Beam

The chamber must be pumped down. The pressure should read below 75mTorr before the filament is turned on. Once the pressure is below the desired range the HV supply is turned on to a voltage between 0 – 5 KV and the filament is turned by increasing the voltage from the variable AC source. The current is then read from the plate to detect a beam hitting the detector plate. A common setting for the beam is one aluminum accelerator grid, 2KV field, and 90VAC. When the beam is running the pressure in the chamber is likely to change, it is good practice to monitor the pressure when the beam is in use.

Setting up the electron beam

1. Turn on the Granville Phillips 275 Mini Convectron thermocouple gauge and vent the chamber to atmospheric pressure.
2. Then remove the Plexiglas lid from the chamber when not under vacuum.
3. Place the beam casing with filament inside of the chamber.
4. Connect the filament with the chambers alligator clips through the *IFT-NW-40-8P* electrical feedthrough (Figure 3b) to a variable AC source “Variac Transformer Model Number TDGC-2KM.”
5. Inside the chamber the aluminum foil that is on the beam casing is then connected with the chamber alligator clips through the *IFT-NW-40-8P* electrical feedthrough (Figure 3b) to the 5kV 3mA positive terminal of a HV power supply “Griffin 5kV EHT Supply.”
6. Connect a wire from the negative 5kV 3mA terminal to one of the wires that connect the variable AC source.
7. Plate the detector plate inside of the chamber and connect with the chambers alligator clips through the *IFT-NW-40-8P* electrical feedthrough (Figure 3b) to a micro ammeter in series to the ground terminal of the HV power supply.
8. Place the lid on the chamber seal the vents and begin to pump down the chamber. The pump switch is towards the back of the chamber on a power strip. Watch on the Convectron pressure gauge as the pressure drops. If the pressure is not dropping, the valve between the pump and the chamber may be shut. If it is open it.
9. Once the chamber pressure reaches ≤ 50 mTorr, turn on the HV power supply and set the voltage to 2kV.
10. Turn on the variable AC source on to about 90 V.
11. Take readings from the ammeter. Adjusting the variable AC source and the HV power supply will produce different results.
12. When data collection is finished turn off the variable AC and HV source. Then slowly vent the chamber to ambient pressure.

The Chamber with Electron Beam Connections